Thermo-Mechanical Analysis of Concrete under Freeze Thaw Test

Hokkaido University　Student member　○Serge EDALO
Hokkaido University　Member　Takashi MATSUMOTO

1. INTRODUCTION

Bridge structures are often subjected to complex thermal stresses which vary continuously with time. The magnitude of these stresses depends on the temperature variation within the structure and this depends on the geographic location and the orientation of the bridge, climatological conditions, cross section geometry and thermal properties of the materials and the exposed surfaces.

In cold and snowing regions, temperature changing from high values to extremely low values and vice versa is very frequent. As a result of that, large temperature gradients are induced causing great thermal stresses in bridge structures located in those areas. Thermal stresses induced in concrete structures can be as large as those produced by dead and live loads[1]. Therefore, thermal stresses can have a significant effect on a structure strength and stability, potentially causing cracks or breaks within certain components. Such failures compromise the overall design of the structure, which can lead to possible weakening.

Thermally induced stresses arise in a heated or cooled structure not directly by the temperature variations themselves, but by restraints of the thermally induced expansions or contractions. These restrictions of the structure movement can come from either external constraints such as displacement constraints, or nonuniform temperature distribution, or a combination of these two causes. In the present study only stresses arising from nonuniform temperature distribution, generally known as primary temperature stresses, have been analyzed.

The objective of this paper is to understand thermally induced stresses occurring in a plain concrete bar under freeze thaw test with the scope of further understanding reinforced concrete (RC) deck slabs in cold regions. Three dimensional finite element analysis is carried out, and thermally induced stresses are discussed in comparison with failure pattern observed in test.

2. GEOMETRY AND MATERIAL PROPERTIES

The analyzed specimen is made of plain concrete and its dimensions consist of 100 mm width, 400 mm length and 100 mm thickness as shown in **Fig. 1**. The specimen stands upright along its length inside a steel container, and rests on the container bottom end plate which is the only contact between the specimen and the container. The specimen is subjected to repeated cycles of heating and cooling. Under the thermal action, the specimen is assumed to freely expand or contract without any restriction. It is also assumed that the water filling the space between the container and the specimen does not restrict the deformation of the specimen. Mechanical and thermal material properties used in this analysis are given in **Table 1**. The values of the table are those recommended par JSCE standard specifications for concrete structures[2].

3. FINITE ELEMENT MODELING

The studied specimen has been modelled using Marc/Mentat finite element analysis software. Three-dimensional approach based on hexahedron solid element is used. The specimen is discretized into cubical elements of size 10 mm. The space bet-

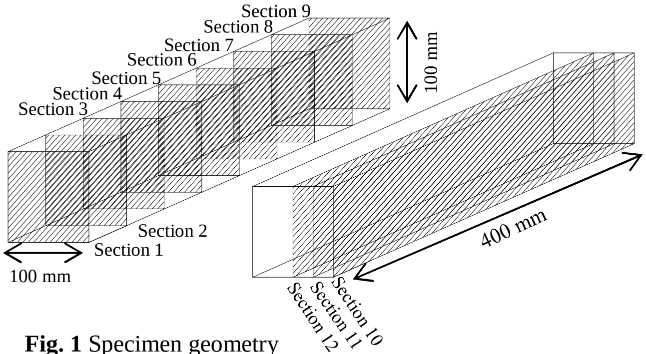

Fig. 1 Specimen geometry

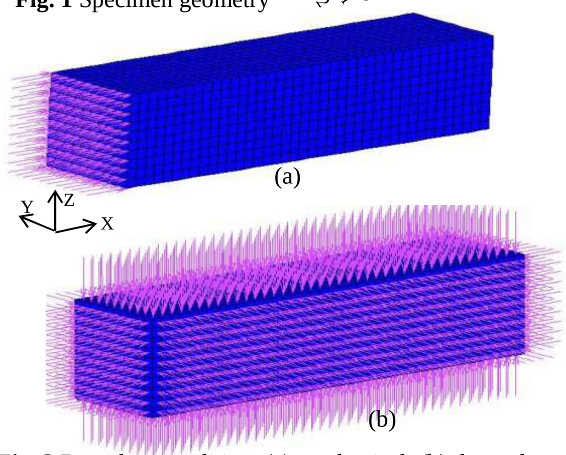

Fig. 2 Boundary condition: (a) mechanical; (b) thermal

Table 1. Material properties[2]

Mechanical properties	Young's modulus	28000 MPa
	Poisson's ratio	0.2
	Density	2400 kg/m^3
Thermal properties	Thermal conductivity	9.2 kJ/mh°C
	Specific heat	1.05 kJ/kg°C
	Thermal expansion coefficient	10^{-5}/°C

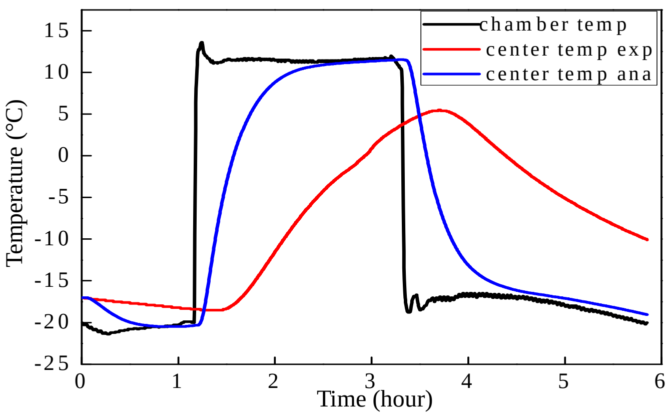

Fig. 3 Temperature variation at specimen center

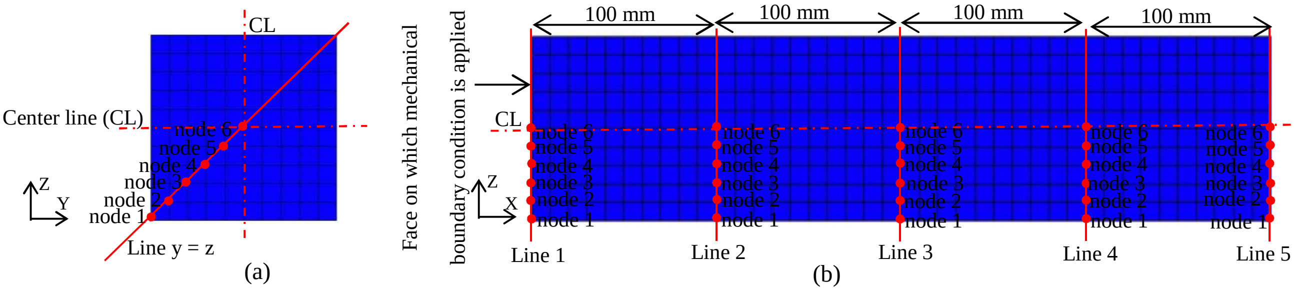

Fig. 4 Lines along which stress is calculated: (a) section 1 to 9; (b) section 10 to 12

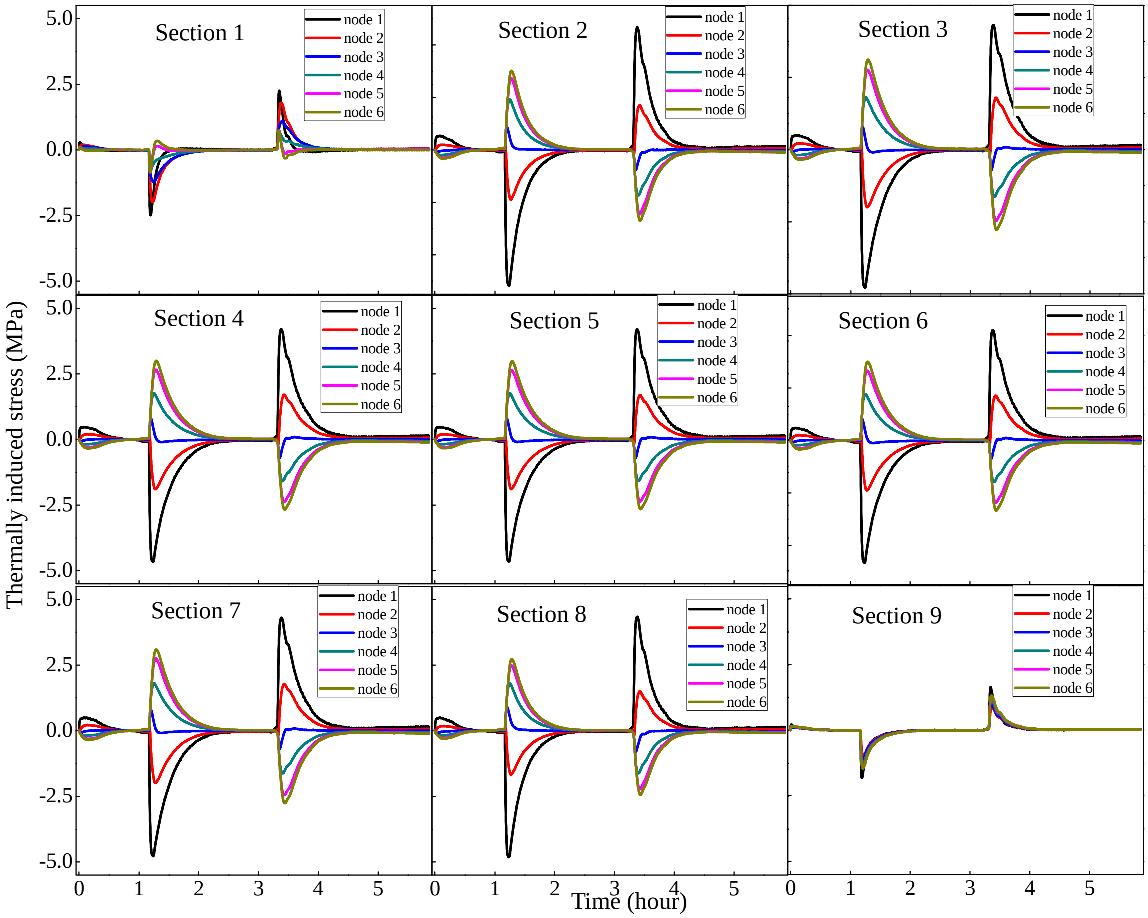

Fig. 5 Time history of thermally induced stress in longitudinal direction (σ_{XX})

-ween the container and the specimen is supposed to be large enough to accommodate all displacements due to thermal action. Therefore, only nodes of elements, the faces of which are resting on the container bottom end plate are fixed in X direction as shown in **Fig. 2** (a). Since the specimen is placed in a chamber where temperature is varied cyclically, the effect of temperature on the specimen is modelled using face film boundary condition with film coefficient of 100 W/m^2°C, and the temperature of the chamber is given as ambient temperature. It is assumed that all specimen faces are subjected to the same temperature action. Therefore, the same thermal boundary condition is applied on all specimen faces as shown in **Fig. 2** (b). An initial temperature of -17°C is applied to all nodes. The analysis is divided in steps, each one corresponding to the temperature change from one magnitude to another.

4. RESULTS

4.1. Temperature at specimen center

The evolution of temperature at the specimen center (x=200 y=50 z=50) is described in **Fig. 3**. One cycle of applied temper-ature represented by the chamber temperature is analyzed. Three major parts can be identified: a transient heating followed by a steady state and then a transient cooling. The temperature at the specimen center given by the numerical analysis reaches faster the steady state than that obtained from the test. This might be due to the value of heat transfer between solid and water which might be a little bit higher. On the whole the temperature at the specimen center obtained by the present numerical analysis suffices to obtain qualitative approximation of the test.

4.2. Thermally induced Stress distribution

To analyze the thermally induced stress, twelve sections have been considered as indicated in **Fig. 1**. For sections ranging from 1 to 9, for each one of them, the thermally induced stress has been calculated at six different nodes. The nodes are numbered from 1 to 6 as shown in **Fig. 4** (a), and they have been chosen along the line of equation y = z since the stress distribution around this line is symmetric. For the rest of the sections, the thermally induced stress has been calculated along five different lines distanced from each other by 100 mm as sh-

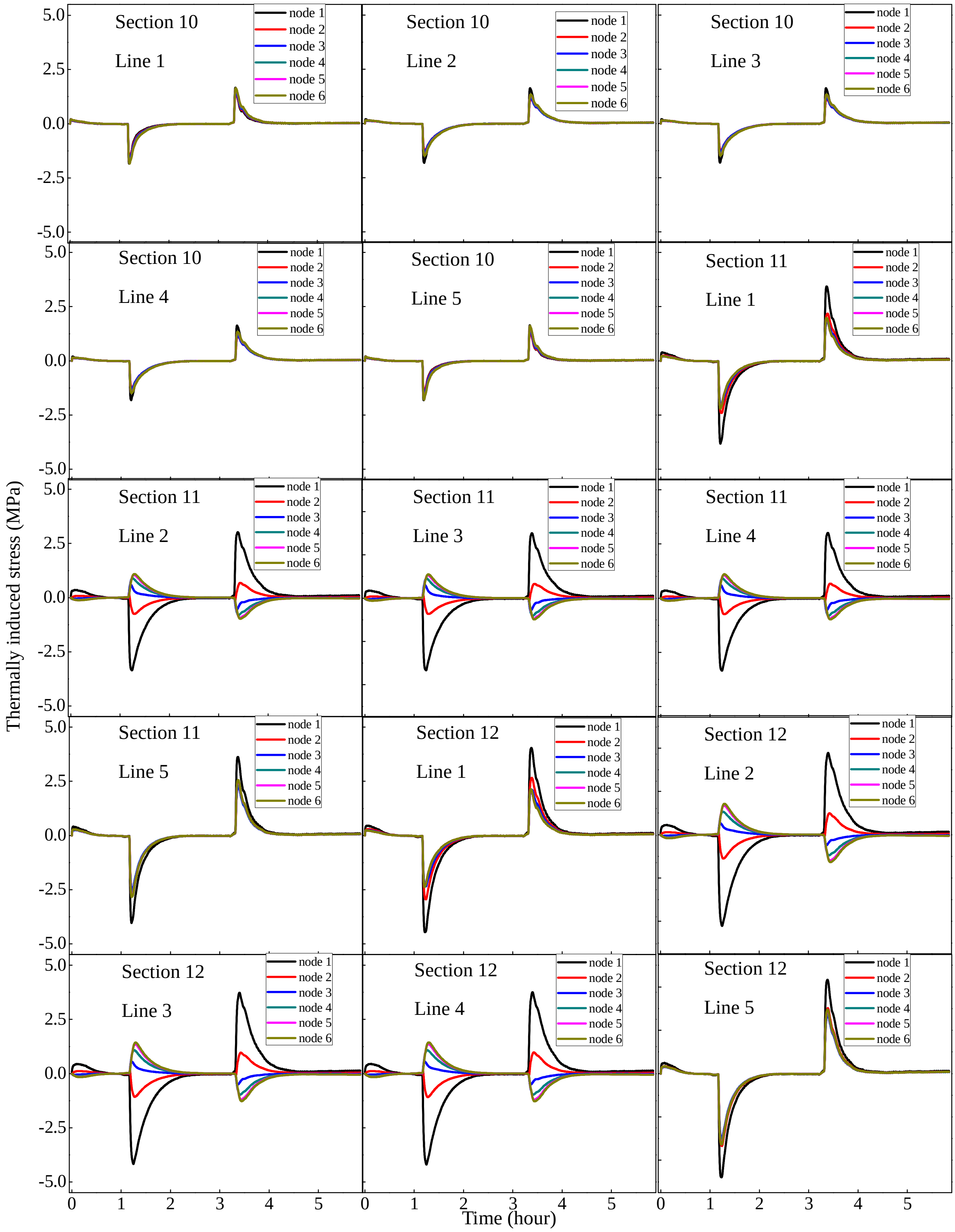

Fig. 6 Time history of thermally induced stress in transverse direction (σ_{YY})

-own in **Fig 4** (b).Along each line, six nodes have also been considered, and they have been also numbered from 1 to 6. Due to symmetry, only a quarter of the specimen is analyzed.

Fig. 5 and **Fig. 6** show the time history of the thermally induced stress respectively in longitudinal direction (σxx) and transverse direction (σ_{YY}). In both directions, two important points are to be noticed: a sudden rising part due to the specimen heating and a sudden dropping part caused by the specimen cooling. During heating of the specimen, while the inner part of the specimen experiences tensile stress, the outer part, on the other hand, undergoes compressive stress. The inv-erse phenomenon is observed when the specimen is cooled. The reason is that the specimen outer and inner part undergo different gradients of temperature[3]. This causes the outer part to expand more than the inner part when the specimen is heated or to contract more than the inner part when the specimen is cooled.

The failure pattern observed in test is shown in **Fig. 7**. At failure, the specimen is broken into two around its middle, and the orientation of the breaking plane indicates that the failure is due to tensile stress acting in longitudinal direction. The result obtained from the carried out analysis is in accord with this fai-

Fig. 7 Specimen failure pattern

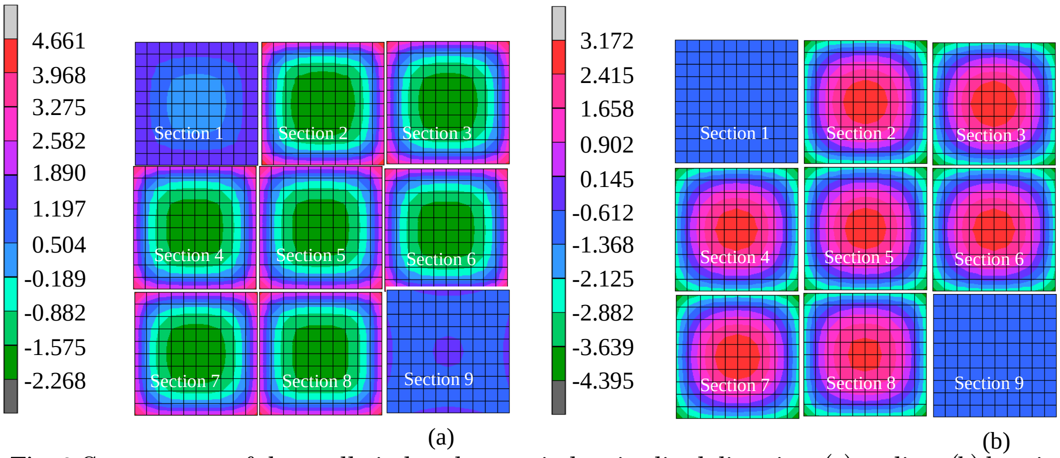

Fig. 8 Contour map of thermally induced stress in longitudinal direction: (a) cooling; (b) heating

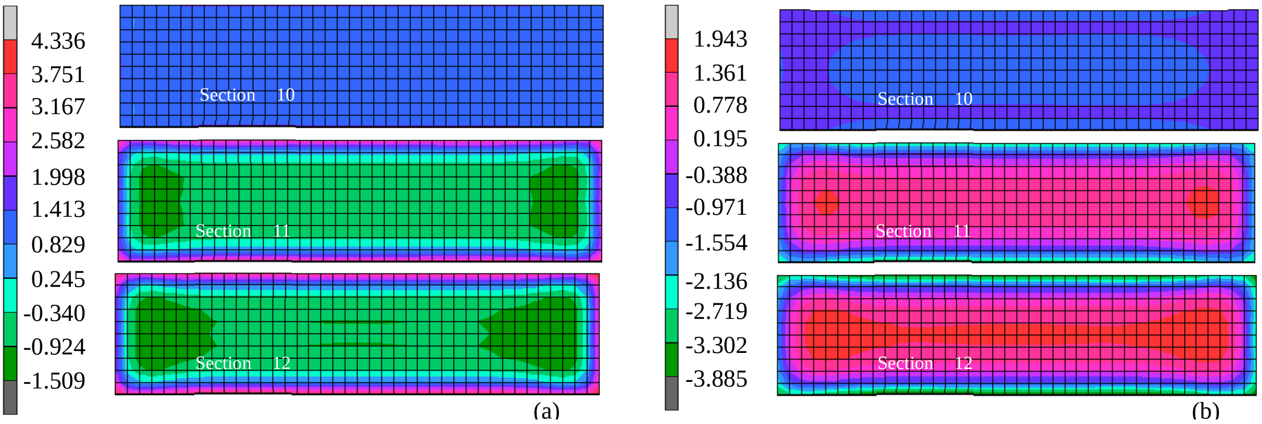

Fig. 9 Contour map of thermally induced stress in transverse direction: (a) cooling; (b) heating

-lure pattern. In fact, the maximum recorded thermally induced tensile stress is in longitudinal direction, and its value which is 4.66 MPa is large enough to provoke crakings in the specimen. Moreover, this maximum value occurs in section 2 not far from the specimen breaking plane.

A close look at tensile stress is provided in **Fig. 8** and **Fig. 9** which show the contour map of the thermally induced stress distribution respectively in longitudinal and transverse direction at increment where the maximum thermally induced tensile stress occurs. During cooling of the specimen, whether it is longitudinal or transverse direction, only the specimen outer part is in tension, and the maximum thermally induced tensile stress decreases when moving from the specimen outer part toward inside the specimen upon a distance about 15 mm. This decreasing can be explained by the fact that during cooling, the specimen outer part contracts more than the inner part, and for Navier-Bernoulli hypothesis that plane section remains plane after deformation to still hold, the outer part must stretch more than the inner part giving rise to decreasing tensile stress[4)]. During heating of the specimen, whether it is longitudinal or transverse direction, only the specimen inner part is in tension, and the maximum thermally induced tensile stress keeps increasing toward the center. This increasing is due to the fact that during heating, the specimen outer part expands more than the inner part, and for Navier-Bernoulli hypothesis that plane section remains plane after deformation to still be true, the inner part must stretch more than the outer part creating thereby increasing tensile stress.

5. CONCLUSION

In this study the thermally induced stress in a specimen made of plain concrete is analyzed. A three dimensional finite element analysis is carried out. It is found that during the specimen heating, while the inner part of the specimen experiences tensile stress, the outer part, on the other hand, undergoes compressive stress. The inverse phenomenon is observed when the specimen is cooled. It is also found that the maximum thermally induced tensile stress is large enough to cause crakings in the specimen, and decreases from the specimen outer part toward inside the specimen upon a distance about 15 mm, and then increases up to the center. Although the degradation of the specimen caused by the water filling the space between the specimen and the container, and its turning into ice during the specimen cooling are not considered in this study, the results obtained, on the whole, reproduce some qualitative trends of the test results.

ACKNOWLEDGEMENT

This is a part of joint research of Civil Engineering Research Institute for Cold Regions, Japan Bridge Association, and Hokkaido University. The authors appreciate the members for the use of test data.

REFERENCES

1) Elbadry, M. M., and Ghali, A.: Control of thermal cracking of concrete structures, ACI Structural Journal, No. 92/4, pp. 435-450, 1995.
2) Standard specifications for concrete structures, JSCE guidelines for concrete, No. 15, p. 503, 2007.
3) Vecchio, F. J., and Sato, J. A.: Thermal gradient effects in reinforced concrete frame structures, ACI Structural Journal, No. 87/3, pp. 262-275, 1990.
4) Priestley, M. J. N.: Design of concrete bridges for temperature gradients, ACI Journal, No 75/5, pp. 209-217, 1978.